EXO70A1-Mediated Vesicle Trafficking Is Critical for Tracheary Element Development in *Arabidopsis*[W][OA]

Shipeng Li,[a,b,c,1] Min Chen,[a,e,1] Dali Yu,[a,c] Shichao Ren,[a] Shufeng Sun,[d] Linde Liu,[f] Tijs Ketelaar,[b] Anne-Mie C. Emons,[b] and Chun-Ming Liu[a,2]

[a] Key Laboratory of Plant Molecular Physiology, Institute of Botany, Chinese Academy of Sciences, Beijing, 100093, China
[b] Laboratory of Cell Biology, Wageningen University, 6708PB Wageningen, The Netherlands
[c] Department of Life Science, Qilu Normal University, Jinan 250013, China
[d] Institute of Biophysics, Chinese Academy of Sciences, Beijing 100101, China
[e] College of Life Science, Shandong Normal University, Jinan 250014, China
[f] College of Life Science, Ludong University, Yantai 264025, China

Exocysts are highly conserved octameric complexes that play an essential role in the tethering of Golgi-derived vesicles to target membranes in eukaryotic organisms. Genes encoding the EXO70 subunit are highly duplicated in plants. Based on expression analyses, we proposed previously that individual EXO70 members may provide the exocyst with functional specificity to regulate cell type– or cargo-specific exocytosis, although direct evidence is not available. Here, we show that, as a gene expressed primarily during tracheary element (TE) development, *EXO70A1* regulates vesicle trafficking in TE differentiation in *Arabidopsis thaliana*. Mutations of *EXO70A1* led to aberrant xylem development, producing dwarfed and nearly sterile plants with very low fertility, reduced cell expansion, and decreased water potential and hydraulic transport. Grafting of a mutant shoot onto wild-type rootstock rescued most of these aboveground phenotypes, while grafting of a wild-type shoot to the mutant rootstock did not rescue the short root hair phenotype, consistent with the role of TEs in hydraulic transport from roots to shoots. Histological analyses revealed an altered pattern of secondary cell wall thickening and accumulation of large membrane-bound compartments specifically in developing TEs of the mutant. We thus propose that EXO70A1 functions in vesicle trafficking in TEs to regulate patterned secondary cell wall thickening.

INTRODUCTION

The tracheary elements (TEs) of xylem tissues in terrestrial plants are elongated and terminally differentiated cells with spiral or pitted secondary cell wall (SCW) thickening (Lucas et al., 2013). The major role of TEs is to transport water and minerals from roots to shoots. TEs are formed through a series of sequential events including cell fate determination, cell elongation, patterned SCW deposition, and programmed cell death (PCD) (Fukuda, 1997; Turner et al., 2007). Exocytosis is expected to occur during patterned SCW thickening in order to insert cellulose synthase complexes into the plasma membrane and to allow deposition of SCW materials, such as hemicellulose and lignin, at specific sites of the cell wall after the cessation of cell elongation (Fukuda, 1997). PCD that occurs during the final stage of TE development removes all intracellular contents and transverse cell walls between adjacent TEs, allowing for unimpeded water movement within mature TEs (Bollhöner et al., 2012). Using in vitro TE differentiation systems of *Zinnia elegans* and *Arabidopsis thaliana*,

two NAC (for NAM, ATAF1,2, CUC2) domain transcription factors, VASCULAR-RELATED NAC-DOMAIN6 and 7, and a transcriptional repressor, VND-INTERACTING2, have been identified as key regulators for TE development (Milioni et al., 2001; Kubo et al., 2005; Yamaguchi et al., 2008, 2010a, 2010b, 2011). A recent study showed that active Rho GTPase ROP11 is able to recruit the MICROTUBULE DEPLETION DOMAIN1 protein to the SCW pits in developing TEs, causing local cortical microtubule disassembly and subsequently preventing the deposition of SCW materials to the pits (Oda and Fukuda, 2012).

In eukaryotic organisms, polarized exocytosis relies on an evolutionarily conserved exocyst complex that consists of eight subunits: SEC3, SEC5, SEC6, SEC8, SEC10, SEC15, EXO70, and EXO84. In budding yeast (*Saccharomyces cerevisiae*), SEC5, SEC6, SEC8, SEC10, SEC15, and EXO84 are associated with vesicles, while SEC3 and EXO70 are localized to the target membranes (Finger et al., 1998; Boyd et al., 2004). Exocysts act downstream of Rho, Rab, and Ral small GTPases to tether secretion vesicles to the target membranes (Robinson et al., 1999; He and Guo, 2009; Wu et al., 2010). As expected, mutations of *SEC3* and *EXO70* in yeast lead to accumulation of secretory vesicles at the budding site (He et al., 2007a).

In many species, such as yeast (*Saccharomyces cerevisiae*) and humans (*Homo sapiens*), each exocyst subunit is encoded by a single gene (Chong et al., 2010). In plants, although most of these exocyst subunits are encoded by one or a few genes, genes encoding for EXO70 are duplicated greatly, with 13 in moss (*Physcomitrella patens*), 15 in grape (*Vitis vinifera*), 23 in *Arabidopsis*,

and 47 in rice (*Oryza sativa*; Cvrčková et al., 2012). Several reports suggest that exocysts in plants are also involved in regulating polarized exocytosis. In *Arabidopsis*, mutations of *SEC5*, *SEC6*, *SEC8*, and *SEC15a* cause defects in pollen germination, pollen tube growth, and pollen transmission (Cole et al., 2005; Hála et al., 2008). Mutations of *EXO84B*, which encodes a cell plate–localized protein, lead to dwarfed plants with defective cytokinesis and accumulation of vesicles in leaf epidermal cells (Fendrych et al., 2010). In maize (*Zea mays*), a mutation in *SEC3* leads to defective root hair elongation (Wen et al., 2005). However, in *Arabidopsis*, although SEC3A–green fluorescent protein has a cell plate localization during cytokinesis, in the tips growing root hairs it forms immobile punctate structures that are evenly distributed over the cell surface, suggesting that it is unlikely involved in polarized secretion (Zhang et al., 2013).

The duplication of *EXO70* genes in plants has received much attention (Elias et al., 2003; Synek et al., 2006; Chong et al., 2010; Zhang et al., 2010; Cvrčková et al., 2012). Because expression of these genes in *Arabidopsis* is diverse and tightly associated with differentiating cells, we proposed previously that individual EXO70 members may provide the exocyst a functional specificity to regulate cell type– or cargo-specific exocytosis. *EXO70C1* that is expressed in guard cells and pollen grains functions in pollen tube growth (Li et al., 2010). Expression of both *EXO70B2* and *EXO70H1* is upregulated by treatment with an elicitor peptide, ELF-18, derived from a bacterial elongation factor. Mutations of these two genes lead to enhanced susceptibility to *Pseudomonas syringae*, thereby implicating roles in plant–pathogen interaction (Pecenková et al., 2011). Recently, it has been shown that a plant U-box type ubiquitin ligase 22 targets EXO70B2 for a pathogen-associated molecular pattern in *Arabidopsis* (Stegmann et al., 2012). EXO70E2 has been implicated in a recently described exocytotic organelle, named EXPO, with unknown functions (Wang et al., 2010).

Microarray and RT-PCR analyses showed that *EXO70A1* is expressed in most organs tested except for mature pollen (Synek et al., 2006; Li et al., 2010). Functions of *EXO70A1* have been implicated in elongation of hypocotyls, stigmatic papillae, and root hairs (Synek et al., 2006), in pollen–stigma interaction during self-incompatibility response (Samuel et al., 2009), in cell plate formation (Fendrych et al., 2010), in pectin deposition in seed coats (Kulich et al., 2010), and in auxin polar transport in root epidermal and cortical cells (Drdováet al., 2013). Using polyclonal antibodies directed against EXO70A1, SEC6, and SEC8 from *Arabidopsis*, Hála et al. (2008) showed that these proteins are colocalized to the apex of growing pollen tubes in tobacco (*Nicotiana tabacum*). Kitashiba et al. (2011) showed that overexpression of EXO70A1 neither abolishes nor weakens self-incompatibility in *Arabidopsis*. Our studies using in situ hybridization and transgenic plants carrying a construct with *EXO70A1* promoter fused with β-glucuronidase (*pEXO70A1*:*GUS*) previously (Li et al., 2010) and in this study showed that *EXO70A1* is not expressed in root hair and cortical cells, pollen grains, pollen tubes, stigmatic papillae, and seed coats, nor during cytokinesis, but primarily in developing TEs. These results prompted us to investigate the role of *EXO70A1* in TE development.

Through genetic, physiological, and cell biological examinations in *Arabidopsis*, we show that EXO70A1 regulates a step between Golgi vesicle production and vesicle fusion during TE development. Mutations of *EXO70A1* in *Arabidopsis* led to nearly sterile and dwarfed plants with reduced cell and organ expansion, decreased water potential, and compromised hydraulic transport. Histological studies revealed that *exo70a1-1* mutants exhibited aberrant xylem with an altered pattern of SCW thickening. Most of these aboveground phenotypes can be rescued by grafting onto a wild-type root stock, while the grafting of a wild-type shoot to the mutant root stock did not rescue the short root hair phenotype. Using cryo-fixation and electron microscopy, we showed that mutation of *EXO70A1* led to altered SCW thickening and accumulation of large membrane-bound vesicles specifically in developing TEs. We thus propose that EXO70A1 acts in cell type–specific exocytosis to regulate TE formation.

RESULTS

EXO70A1 Is Primarily Expressed in Developing TEs

Using in situ hybridization, in transgenic plants carrying a *GUS* reporter construct, we showed previously that *EXO70A1* is expressed during TE development (Li et al., 2010). In this study, we performed further analyses on *pEXO70A1*:*GUS* transgenic plants and confirmed that, in all tissues examined, *GUS* expression was observed specifically in differentiating TEs (Figure 1). Within the vascular bundles of roots (Figures 1A and 1B), cotyledons (Figure 1C), and leaves (Figure 1D), weak *GUS* expression was first observed in elongated TEs before patterned SCW thickening became visible (Figures 1A and 1C, white arrowheads), and *GUS* expression became stronger when patterned SCW thickening formed (Figures 1A to 1D, black arrowheads). *GUS* expression was most abundantly observed when patterned SCW thickening was distinct (Figures 1A and 1C, black arrows) and disappeared gradually afterwards. No *GUS* expression was seen in mature TEs (Figures 1B to 1D, white arrows). The association of *GUS* expression with developing TEs was observed in all organs examined: young hypocotyls (see Supplemental Figure 1A online), inflorescence stems (see Supplemental Figure 1B online), and pedicels (see Supplemental Figure 1C online). Although defective root hair elongation, pollen rehydration, and seed coat pectin deposition have been reported in *exo70a1* mutants (Synek et al., 2006; Samuel et al., 2009; Kulich et al., 2010), we did not detect *GUS* expression in root hairs, pollen grains, stigmatic papillae, or seed coats in the stages we examined.

Mutations of *EXO70A1* Lead to Dwarfed and Nearly Sterile Plants with Reduced Water Potential

To elucidate the function of *EXO70A1*, two independent insertion lines from the SALK collection (www.Arabidopsis.org), namely, *exo70a1-1* and *exo70a1-2*, with T-DNAs inserted in the first intron and the sixth exon, respectively, were examined. Consistent with results published previously, phenotypes of these two alleles are similar to each other (Synek et al., 2006). Therefore, in the following studies, we focused on *exo70a1-1*, as it has been shown to be a null allele (Synek et al., 2006). Homozygous *exo70a1-1* plants were dwarfed and nearly sterile with smaller leaves, compared with the wild type (Figure 2A; see Supplemental
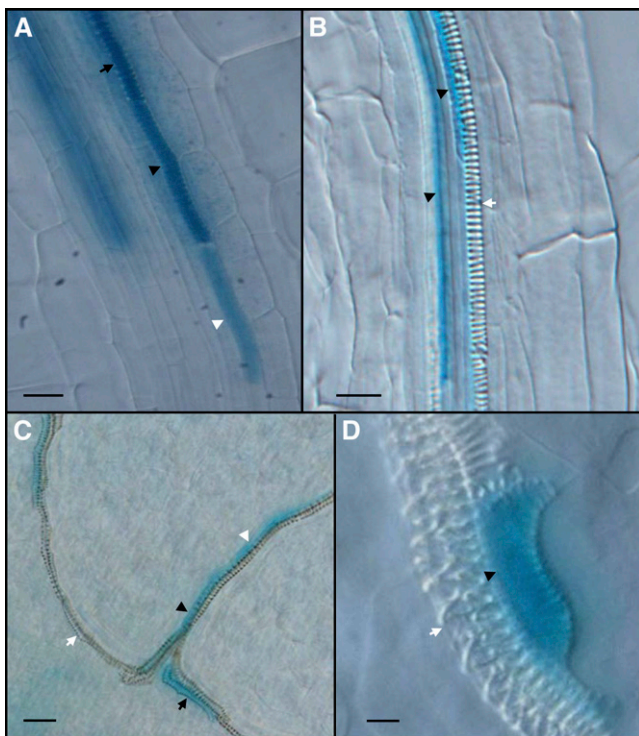
Figure 1. *EXO70A1* Is Primarily Expressed in Developing TEs.

(A) to **(C)** In 5-d-old *Arabidopsis* seedlings carrying *pEXO70A1:GUS*, *GUS* expression was observed in differentiating TEs in young **(A)** and mature roots **(B)** and in cotyledons **(C)**. Note that weak *GUS* expression was observed in the elongating TE (white arrowhead), stronger expression was observed in the TE when the spiral patterned SCW thickening was visible (black arrowheads), and the strongest *GUS* expression in the TE was observed when the spiral patterned SCW thickenings were distinct (black arrow).
(D) In leaves of 10-d-old *pEXO70A1:GUS* seedlings, *GUS* expression was observed in TEs during the patterned SCW thickening (black arrowhead) but absent in mature TEs (white arrow).
Bars = 20 μm in **(A)**, **(B)**, and **(D)** and 50 μm in **(C)**.

Figure 2 online). The average areas of fully expanded fifth leaves in the wild type were measured as 114.09 $\pm$ 13.32 mm^2 (*n* = 14), while those in *exo70a1-1* were 35.84 $\pm$ 8.49 mm^2 (*n* = 14; P < 0.01, as determined by Student's *t* test). In normal growth conditions, in contrast with over 1000 seeds produced from each wild-type plant, <10 seeds were produced in a full-grown *exo70a1-1* plant. Both the floral buds (stage 12, just before flower opening; Smyth et al., 1990; Figure 2B, top panel) and open flowers (stage 13; Figure 2B, bottom panel) in *exo70a1-1* were smaller than those in the wild type, with shorter sepals, petals, and pistils, as reported previously (Synek et al., 2006).

To address possible physiological defects in *exo70a1-1*, we examined water content, water loss rate, and water potential. Leaves of *exo70a1-1* plants had both significantly lower water content (Figure 2C) and reduced water potential (Figure 2D) compared with those in the wild type (P < 0.01, as determined by Student's *t* test). We also observed a reduced water loss rate

in *exo70a1-1* leaves (Figure 2E). These studies suggest a possible defect in hydraulic transport in the mutant.

We measured the mineral content in aboveground tissues (mixed harvested samples of leaves, stems, flowers, and siliques) using inductively coupled plasma–mass spectrometry (ELAN DRC-e; Perkin-Elmer) and found no apparent differences between *exo70a1-1* and the wild type (see Supplemental Figure 3 online), suggesting the mutant phenotype is unlikely to be caused by nutritional defects.

Mutation of *EXO70A1* Leads to Reduced Cell Expansion

Consistent with the observation from Synek et al. (2006), *exo70a1-1* seedlings grown on culture plates exhibited shorter root hairs compared with the wild type (Figure 3A). In transversely sectioned roots, hypocotyls, and stems, reduced cell expansion was observed in almost all of the cell types in *exo70a1-1* compared with those in the wild type (Figures 3B and 3C; see Supplemental Figures 4A to 4F online). The diameters of individual TEs in both protoxylem and metaxylem in transversely sectioned *exo70a1-1* roots were smaller than those in the wild type (Figures 3D and 3E). In addition, extra cell division was observed in both pericycle and ground tissue in *exo70a1-1* (Figures 3D and 3E, arrowheads).

The *exo70a1-1* plants also showed smaller floral organs. In fully opened stage 13 flowers, the lengths of sepals, petals, and pistils in the wild type were measured as 1618.2 $\pm$ 138.48 μm, 1762.36 $\pm$ 249.06 μm, and 1835.65 $\pm$ 119.51 μm, respectively; while those in *exo70a1-1* were 656.12 $\pm$ 126.09 μm, 688.85 $\pm$ 85.69 μm, and 434.3 $\pm$ 50.83 μm, respectively (*n* = 15 for each measurement; P < 0.01 for every comparative pair, as determined by Student's *t* test). We then examined the lengths of cells in petals excised from these flowers. Under a differential interference contrast (DIC) microscope, we observed that, although cell sizes in the upper portion of the petal in *exo70a1-1* were similar to those in the wild type, cell lengths in the lower portion of the petal from *exo70a1-1* were significantly reduced (Figure 3F). Such a difference was not observed in these cells prior to flower opening. Therefore, it is likely that the shorter petal phenotype observed in *exo70a1-1* was caused by reduced cell elongation in this region.

The Nearly Sterile Phenotype of *exo70a1-1* Was Rescued by Grafting

To examine the *exo70a1-1* phenotype further, we performed grafting experiments. We switched the shoots and roots between wild-type and *exo70a1-1* plants by cutting and joining shoots and roots at the hypocotyl position of 3-d-old seedlings. Grafted seedlings were maintained under sterile conditions for 7 d before being transferred to soil. We used the naming convention "rootstock-scion" to describe grafted plants. Therefore, "W-m" is used for plants with an *exo70a1-1* shoot grafted onto a wild-type root and "m-W" for a wild-type shoot grafted onto an *exo70a1-1* root. "W-W" and "m-m" refer to self-grafts of the wild type and the *exo70a1-1*, respectively. In the W-W and m-m graftings, plants obtained were almost indistinguishable from those nongrafted ones, suggesting that the grafting did not affect their general growth and development (Figure 2A). Following transfer to soil, slightly dwarfed plants with normal seed set were
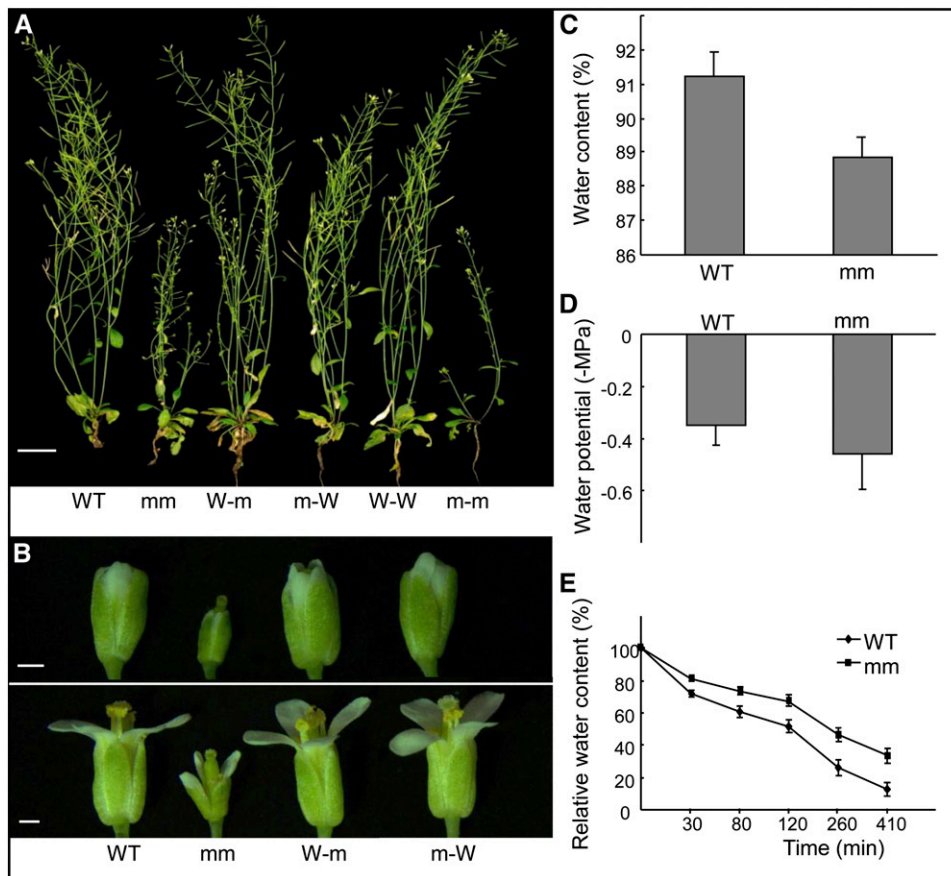
Figure 2. Most Defects in Aerial Parts of *exo70a1-1* Were Rescued by Grafting onto Wild-Type *Arabidopsis* Rootstock.

(A) Fifty-day-old plants, with or without grafting, showing the phenotypes of wild-type (WT) and mm plants and plants from different grafting combinations, as described below. The dwarf and nearly sterile phenotypes of *exo70a1-1* were partially rescued by the W-m grafting. Bar = 4 cm.
(B) Floral buds and open flowers from the wild-type, mm, and W-m and m-W grafted plants, showing that the W-m grafting led to normal organ expansion in the *exo70a1-1* flower. Bars = 0.5 mm.
(C) Water content in the wild-type and mm leaves. Values are means ± sd (*n* = 15), with significant difference as determined by Student *t* test, P < 0.01.
(D) Water potential in wild-type and mm plants. Water potential was measured using a thermocouple psychrometer. Values are means ± sd (*n* = 20), with significant difference as determined by the Student *t* test, P < 0.01.
(E) Water loss rates in the wild-type and mm leaves. Data represent the means ± sd of four biological replicates (*n* = 20).
mm, homozygous *exo70a1-1*; graft combinations (rootstock-scion): W-W, a wild-type scion onto a wild-type rootstock; m-m, an *exo70a1-1* scion onto an *exo70a1-1* rootstock; W-m, an *exo70a1-1* scion onto a wild-type rootstock; m-W, a wild-type scion onto an *exo70a1-1* rootstock.

obtained from m-W seedlings (Figure 2A), suggesting that the grafted *exo70a1-1* root caused only a slight growth retardation to the wild-type shoot. By contrast, W-m grafted plants, when compared with *exo70a1-1* plants, showed greatly restored growth and fertility (Figure 2A). Seed set in primary inflorescences of W-m plants was similar to that of the wild type, while in secondary branches, a reduced seed set was observed (Figure 2A, arrow), suggesting that the wild-type root is able to partially rescue the growth and fertility defects in *exo70a1-1*.

We next examined whether grafting could rescue the small floral organ phenotype in *exo70a1-1*. In the main inflorescence of W-m grafted plants, the sizes of stage 12 floral buds and stage 13 flowers were indistinguishable from those of the wild type (Figure 2B), suggesting that expansion of these organs in *exo70a1-1* flowers are restored by the grafted wild-type root.

However, in side branches where the nearly sterile phenotype was evident, the sizes of floral buds and flowers were about the same as those in *exo70a1-1*, suggesting a close connection between organ expansion and fertility. In m-W grafted plants, the sizes of floral buds and flowers showed no difference from those in the wild type (Figure 2B).

When m-W seedlings were grown on vertically cultured plates, we observed that these seedlings still exhibited short root hairs (Figure 3A). Moreover, in W-m grafted seedlings, normal root hairs were observed (Figure 3A). Thus, it is unlikely that the short-root hair phenotype was caused by disrupted nutrients or signals from the shoot.

We then measured cell lengths in the lower portion of the petal in different grafting combinations and observed that epidermal cell lengths were increased significantly in W-m grafted plants
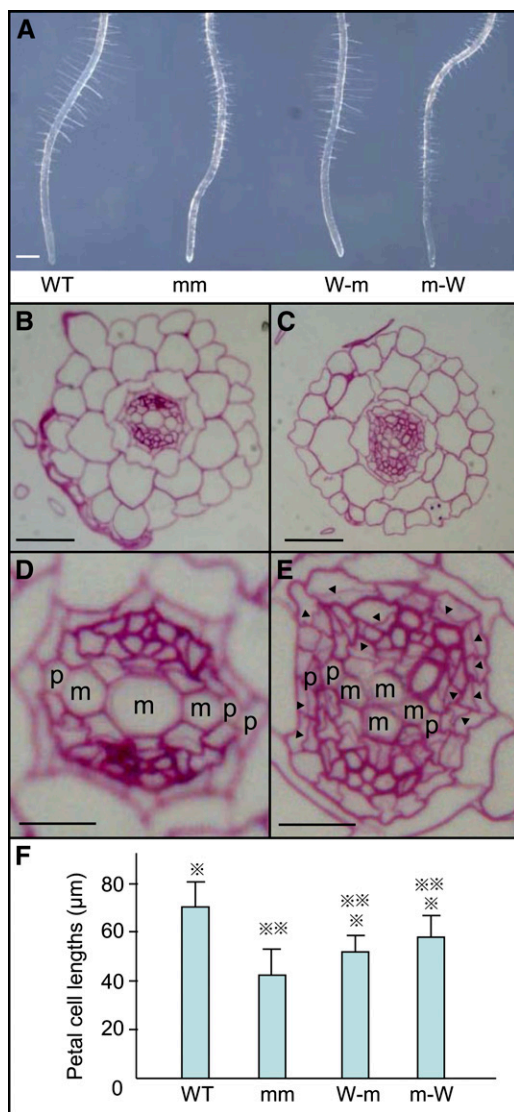
Figure 3. Defective Cell Expansion in *exo70a1-1*.

(A) The *exo70a1-1* root (mm) exhibits shorter root hairs compared with wild-type (WT) *Arabidopsis*. The phenotype was not rescued by the m-W grafting (rootstock-scion). No short-root hair phenotype was observed in the W-m grafted plants.

(B) and **(C)** Periodic Acid-Schiff staining of transverse sections of mature roots from 10-d-old wild-type **(B)** and *exo70a1-1* **(C)** seedlings.

(D) and **(E)** Enlarged images of **(B)** and **(C)**, respectively. Note the reduced sizes of both protoxylem (p) and metaxylem (m) and extra cell divisions (indicated by arrowheads) in pericycle and ground tissues.

(F) Lengths of epidermal cells in open flowers. Cells at the abaxial side and basal part of the petal were measured. Values are means ± 1 SD (n = 24), single asterisks represent significant differences from the *exo70a1-1* (mm), and double asterisks represent significant differences from the wild type as determined by Student's *t* test, P value < 0.05.

Bars = 250 μm in **(A)**, 25 μm in **(B)** and **(C)**, and 10 μm in **(D)** and **(E)**.

compared with those in homozygous *exo70a1-1* (mm; Figure 3F), suggesting that elongation of these cells was restored by the wild-type rootstock. We did notice that cells in W-m and m-W grafted plants were still significantly shorter than those in the wild type (Figure 3F), indicating that the cell elongation in both graftings did not achieve the same level as that in the wild type. Since the lengths of the flowers in both grafting combinations were about the same as those of the wild type, it is plausible that extra cell divisions in petals of these grafted plants compensated for the reduced cell elongation.

It has been reported previously that the stigmatic papillae in *exo70a1-1* is immature in appearance, with almost no elongation (Synek et al., 2006). We examined if grafting could rescue this phenotype. As showed in Supplemental Figure 5 online, the elongation of stigmatic papillae in open flowers of W-m grafted plants was about the same as those in W-W grafting, while those in m-m grafting had no elongation, as with those in the *exo70a1-1* mutant. This result showed the W-m grafting restored the defective stigmatic papillae elongation in *exo70a1-1*.

These grafting experiments together revealed that the grafted wild-type root is able to repair most defects in the aboveground organs of *exo70a1-1* plants, such as cell expansion and fertility. Most likely the reduced cell expansion in *exo70a1-1* is caused by defective root to shoot hydraulic transport, while the reduced root hair elongation is not caused by defects in shoots.

The Nearly Sterile Phenotype of *exo70a1-1* Is Caused by Defects in Pollination

Based on defective pollen rehydration on stigmas in *exo70a1-1* mutants and *Exo70A1RNAi* transgenic *Brassica napus* plants, it has been proposed previously that *EXO70A1* is involved in the self-incompatibility response (Samuel et al., 2009). We examined whether or not this supposition is true. Although *exo70a1-1* plants produced very few pollen grains, we were able to perform hand-pollination experiments with pollen from several anthers. When wild-type pollen was used to pollinate *exo70a1-1* stigmas, ~45% of siliques (n = 20) were able to expand to the length of the wild-type ones after 4 d, and 10 to 30 seeds were produced in each silique. Similarly, when wild-type stigma were pollinated by *exo70a1-1* pollen, 65% of siliques (n = 20) were able to expand to the length of the wild-type ones, producing 20 to 40 seeds in each silique. When *exo70a1-1* pistils were hand-pollinated with self pollen, we observed that up to 20 seeds per silique were produced. All progeny obtained from the self-pollination were homozygous for the T-DNA insertion, as shown by PCR-based genotyping, and exhibited *exo70a1-1* phenotypes, thereby excluding the possibility of pollen contamination. Most likely the nearly sterile phenotype is caused by a mechanistic defect in pollination. Consistent with this observation, aniline blue staining of pistils from *exo70a1-1* flowers 1 d after anthesis revealed almost no pollen tubes in the style (Figure 4B), while a large number of pollen tubes was observed in the style of the wild type (Figure 4A). The number of pollen tubes in the mutant style was increased significantly when *exo70a1-1* stigma was hand-pollinated with self-pollen (Figures 4C and 4D). Thus, it is plausible that the nearly sterile phenotype in *exo70a1-1* is caused by failure in pollination through combined defects in male and female floral organs.

Mutation of *EXO70A1* Leads to Reduced Hydraulic Conductance

To address if hydraulic transport was affected in *exo70a1-1*, we designed an ink transport experiment. Young inflorescence stems, 2 cm in length, were excised from wild-type and *exo70a1-1* plants, in which all postanthesis siliques were removed, keeping flowers and floral buds intact. The bottom ends of the inflorescence stems were soaked in 1:5 diluted red or blue ink. Using a dissection microscope, we monitored how long it took for the ink to reach the sepals and petals. As shown in Figure 5, the ink was visible in the sepals and petals from the wild-type in ~40 min, while it took ~120 min to reach the flower in the *exo70a1-1*. Unexpectedly, neither inflorescence stems excised from the m-W grafted nor those from the W-m grafted plants showed altered hydraulic transport efficiencies compared with inflorescence stems with the same genotype from nongrafted plants, suggesting that the restored fertility and organ expansion observed in aboveground organs in *exo70a1-1* after grafting are not caused by improved hydraulic conductance in inflorescence stems.

To examine if hydraulic transport is also compromised in the root of *exo70a1-1* plants, we designed an ink transport experiment for roots. We monitored how long it took for the ink to move from the 2-cm-long roots to the hypocotyl under a dissection microscope. As shown in Figure 5C, the average time needed for the ink to reach the hypocotyl was 3.28 ± 0.56 h for the wild type, while it was 8.44 ± 2.13 h for the *exo70a1-1* plants ($n = 30$; $P < 0.01$, as determined by Student's t test), suggesting a compromised hydraulic transport in the root of *exo70a1-1*.

These studies together revealed that the hydraulic transport efficiencies in the inflorescence stems and roots of *exo70a1-1* have been reduced to approximately one-third of those in the wild type.

exo70a1-1 Mutants Show Irregular TE Development

TEs in *Arabidopsis* exhibit highly organized patterns of SCW deposition, which is spiral-shaped in the protoxylem and pitted in the metaxylem. In addition to the aforementioned reduced inner diameter of TEs in both protoxylem and metaxylem in transversely sectioned *exo70a1-1* roots (Figures 3D and 3E), we also observed that the inner diameter of TEs in *exo70a1-1* was greatly reduced in transversely sectioned inflorescence stems (Figures 6A and 6B). We then examined whether the mutation of *EXO70A1* led to altered TE development. In cleared samples, we observed that basic TEs were present in *exo70a1-1* inflorescences. However, in stage 13 flowers, we noticed that TEs in pistils were very faint in *exo70a1-1* compared with those in the wild type (Figures 6C and 6D). Similarly, TEs with variable thickness were observed in the inflorescence stems of *exo70a1-1* (Figures 6E and 6F).

More detailed studies were performed at the seedling stage. We observed that TEs in *exo70a1-1* cotyledons often exhibited discontinuity, with alternations of strong and weak light reflections as observed under a DIC microscope (Figures 7A and 7B). Similar defects were also observed in hypocotyls (see Supplemental Figure 6 online). The altered TE morphology was more evident in seedlings stained with basic fuchsin in which lignin-containing TEs were bright pink (Figures 7C and 7D). Confocal microscopy observations of propidium iodide–stained root samples revealed that, instead of the well-organized pits in the metaxylem of the wild type, irregular patterns of pits with variable distances between them were observed in *exo70a1-1* plants (Figures 7E and 7F). Although the length of mature TEs in *exo70a1-1* roots was not significantly different from those in the wild type, a significantly reduced inner diameter of TEs was observed (Table 1). The width of perforations between two neighboring TEs was also narrower in *exo70a1-1* than those in the wild type (Figures 7G and 7H, Table 1). Among 47 TEs examined in *exo70a1-1*, five of them showed an absence of perforations.

We then used transmission electron microscopy (TEM) to examine the junction regions between cotyledons and the hypocotyl, where TE differentiation is active. Instead of the regularly patterned SCW thickening in the wild type (Figure 7I), we observed various shapes of SCW thickening and irregular distances between neighboring thickening within mature TEs in *exo70a1-1* (Figure 7J). Furthermore, the distances between two neighboring SCW thickenings were significantly larger than those in the wild type (Table 1; $n = 150$, $P < 0.01$, as determined by Student's t test). Also, patterned SCW thickening was often
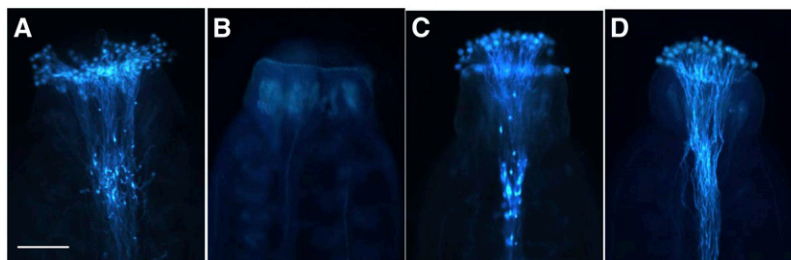

Figure 4. In Vivo Pollen Germination.

Pollen tubes in styles were visualized under a florescence microscope after aniline blue staining. Bar = 100 μm for all photos.
(A) A self-pollinated wild-type *Arabidopsis* pistil.
(B) A self-pollinated *exo70a1-1* pistil. Note that no pollen tube was observed in the style.
(C) A wild-type pistil was hand-pollinated with self pollen.
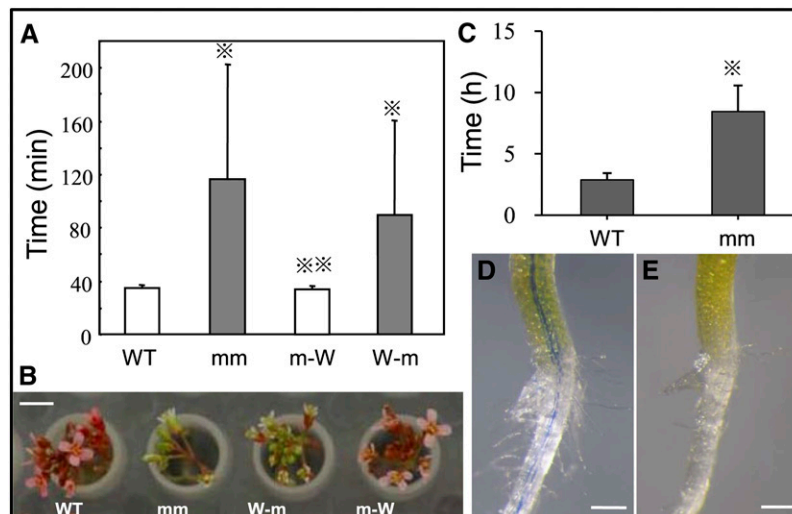**(D)** An *exo70a1-1* pistil was hand-pollinated with self pollen.

Figure 5. Ink Transport in *Arabidopsis* Inflorescences and Roots.

(A) Ink transport in inflorescences. Time needed for ink to reach the first flower. Values are means ± SD (*n* = 24). Note it took ~3 times longer time for the ink to reach flowers for *exo70a1-1* (mm) than that in the wild type. No significant differences were observed between the wild-type (WT) and m-W inflorescences nor between the *exo70a1-1* and W-m inflorescences. Values are means ± SD (*n* = 10). Single asterisks represent significant differences from the wild-type, while the double asterisk represents a significant difference from the *exo70a1-1* (mm), as determined by the Student's *t* test, P value < 0.05.

(B) Ink transported to flowers. Pictures were taken 2 h after soaking the bottom ends of inflorescences in the ink. Bar = 3 mm.

(C) Ink transport in roots. Time needed for ink to be transported from root tips to bottom ends of hypocotyls in 8-d-old seedlings (*n* = 30). The distance for ink transport is 2 cm for both the wild type and the *exo70a1-1*. The asterisk represents a significant difference between the wild type and the mutant, as determined by the Student's *t* test, P value < 0.01.

(D) and **(E)** Ink transported from roots to hypocotyls. Photographs were taken 4 h after the test started, showing the blue ink in vascular bundles of hypocotyl of the wild type **(D)** but not in *exo70a1-1* **(E)**. Bars = 200 μm.

observed at the perforation sites in the *exo70a1-1* plants (six out of 11 examined), leading to narrow perforations (see Supplemental Figure 7 online). It is interesting to note that the PCD that occurs during the final stage of TE development to remove cellular contents does not seem to be affected by the mutation of *EXO70A1* (Figures 7I and 7J).

Membrane-Bound Compartments Accumulate in Developing TEs of *exo70a1-1*

We used high-pressure cryo-fixation in combination with TEM to examine TE development at the junction regions between cotyledons and the hypocotyl. We focused our attention on developing TEs in which the patterned SCW thickening was evident. In the wild-type plants during patterned SCW deposition in TEs, we observed Golgi vesicles with an average size of 75.1 ± 12.98 nm (*n* = 50; Figures 8A and 8E). However, in developing TEs of *exo70a1-1* plants, we observed that Golgi bodies in the *exo70a1-1* were often deformed, with an increased number of cisternae (Figure 8D). The average number of Golgi cisternae in developing TEs in wild-type plants was 3.75 ± 0.55, while the average number in *exo70a1-1* plants was 5.10 ± 0.79 (*n* > 20, P < 0.01, as determined by Student's *t* test). More strikingly, we observed abundant accumulation of larger membrane-bound compartments with an average size of 158.97 ± 46.44 nm (*n* = 53) in the cytoplasm of developing TEs in *exo70a1-1* plants (Figures 7B and

7F), a size that is significantly different from those Golgi vesicles observed in the wild type (P < 0.01, as determined by Student's *t* test). In the surrounding non-TE cells, these abnormal Golgi bodies and large membrane-bound compartments were not observed, suggesting that the defect is specific to TEs. Since these accumulated membrane-bound compartments were much larger than normal Golgi vesicles, we speculate that they either originate from fusions of multiple vesicles or that the mutation of *EXO70A1* leads to the production of larger vesicles.

DISCUSSION

Instead of one gene encoding each subunit of the octomeric exocyst complex as in most animal species, genes encoding EXO70 in plants are expanded greatly for unknown reasons. As the most well-characterized member of the 23 EXO70s in *Arabidopsis*, the functions of EXO70A1 have been implicated in hypocotyl and root hair elongation (Synek et al., 2006), self-incompatibility (Samuel et al., 2009), cytokinesis (Fendrych et al., 2010), localized pectin deposition in seed coat (Kulich et al., 2010), and auxin polar transport in roots (Drdová et al., 2013). However, our expression studies showed that *EXO70A1* is primarily expressed in developing TEs (Li et al., 2010). In this study, we showed by combined genetic, physiological, histological, and grafting experiments that EXO70A1 regulates vesicle trafficking
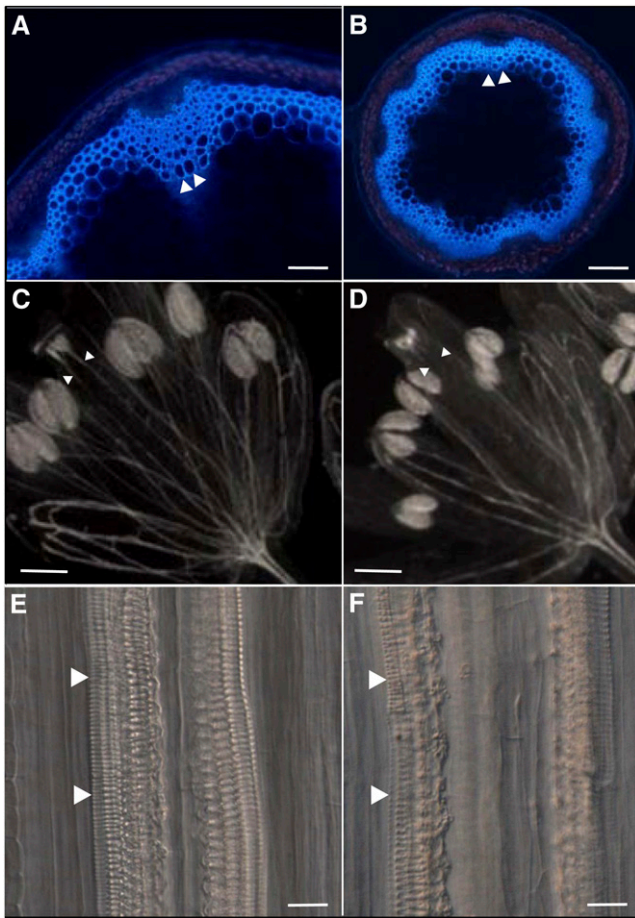
Figure 6. Defective TE Formation in *exo70a1-1*.

(A) and **(B)** UV autofluorescence of transversely sectioned inflorescence stems of the wild type **(A)** and *exo70a1-1* **(B)**, showing smaller TEs (arrowheads) in *exo70a1-1* compared with those in the wild-type *Arabidopsis*.

(C) and **(D)** Dark-field observations of the wild-type **(C)** and *exo70a1-1* **(D)** stage 13 flowers. Note the underdeveloped TEs (arrowheads) in the pistils of *exo70a1-1* pistils compared with those in the wild type.

(E) and **(F)** Abnormal TEs observed in cleared *exo70a1-1* inflorescence stems. Note the difference between TEs in the wild type (**[E]**, indicated by arrowheads) and those in *exo70a1-1* (**[F]**, arrowheads).

Bars = 500 μm in **(A)** and **(B)**, 40 μm in **(C)** and **(D)**, and 100 μm in **(E)** and **(F)**.

during patterned SCW thickening in developing TEs, supporting our hypothesis that individual EXO70s in plants may regulate cell type–specific exocytosis.

EXO70A1 Is Specifically Expressed in Developing TEs

Xylem consists of interconnecting TEs, which build long-distance capillary channels to deliver water and minerals from roots to aerial parts of the plant (Lucas et al., 2013). TE development involves a series of developmental events including cell elongation, patterned SCW reinforcement, PCD, and perforation of walls between joint TEs. Patterned SCW thickening adds strength

and rigidity to mature TEs to prevent collapse under the high negative pressures exerted by transpiration (Fukuda, 1997, 2004; Turner et al., 2007). Patterned SCW deposition in TEs usually occurs at the lateral cell faces and is excluded from the end walls that become perforated during the final stage of TE development. Particle rosettes, now known to be cellulose synthase complexes (Kimura et al., 1999), have been observed in vesicles of differentiating TEs in *Zinnia* decades ago (Haigler and Brown, 1986), suggesting exocytosis is involved in SCW thickening (Fukuda, 1997; Ye, 2002; Turner et al., 2007).

EXO70A1 has been implicated in hypocotyl and root hair elongation (Synek et al., 2006), self-incompatibility (Samuel et al., 2009), and localized deposition of seed coat pectin (Kulich et al., 2010). The expression data used in these studies are mainly from the publicly available Genevestigator database, showing that *EXO70A1* is expressed in all tissue samples examined except for mature pollen (Synek et al., 2006; Kulich et al., 2010). However, our expression analyses using *pEXO70A1:GUS* transgenic plants revealed that, as verified by in situ hybridization, *EXO70A1* is one of two *EXO70* genes in *Arabidopsis* expressed in developing TEs (Li et al., 2010). Here, we further showed that *EXO70A1* is primarily expressed in developing TEs in roots, hypocotyls, cotyledons, leaves, stems, and various floral organs. Within TEs, the expression was first observed during TE elongation, then became stronger during patterned SCW thickening, and ceased completely in mature TEs. No expression was observed in root hairs, pollen grains, stigmatic papillae, or seed coats in the stages examined. Since TEs are a specialized tissue running across almost all organs, the expression profile established in whole-organ level microarray analyses is true but can be misleading when interpreted improperly. We therefore propose that, although microarrays are an efficient tool to provide a general picture for gene expression, it is critically important to use in situ hybridization and reporter constructs to elucidate the expression pattern at the cellular level when individual genes are studied.

Most Defects Observed in *exo70a1-1* Can Be Explained by Imperfect TEs

Homozygous *exo70a1-1* plants show pleiotropic phenotypes, including dwarfing, shortened root hairs, and greatly reduced fertility (Synek et al., 2006; Samuel et al., 2009). Genetic analyses showed that pollen in *exo70a1* functions normally, while the reduced fertilization and seed set are caused by a sporophytic defect (Synek et al., 2006). We showed that both the pollen tube growth in styles and seed set were improved greatly in *exo70a1-1* when hand-assisted pollinations were performed, indicating a mechanistic defect in pollination. This is further supported by the observation that, when wild-type roots were grafted to *exo70a1-1* shoots, the mutant shoots showed an almost complete restoration of stigmatic papillae elongation and seed set.

Physiological experiments performed here revealed that *exo70a1-1* plants exhibited significantly reduced water content, water potential, and water loss efficiency. Analyses of mineral content in aboveground tissues of *exo70a1-1* plants did not show significant differences from those of the wild type. However, histological studies showed reduced cell expansion in many cell types throughout the *exo70a1-1* plant (Synek et al.,
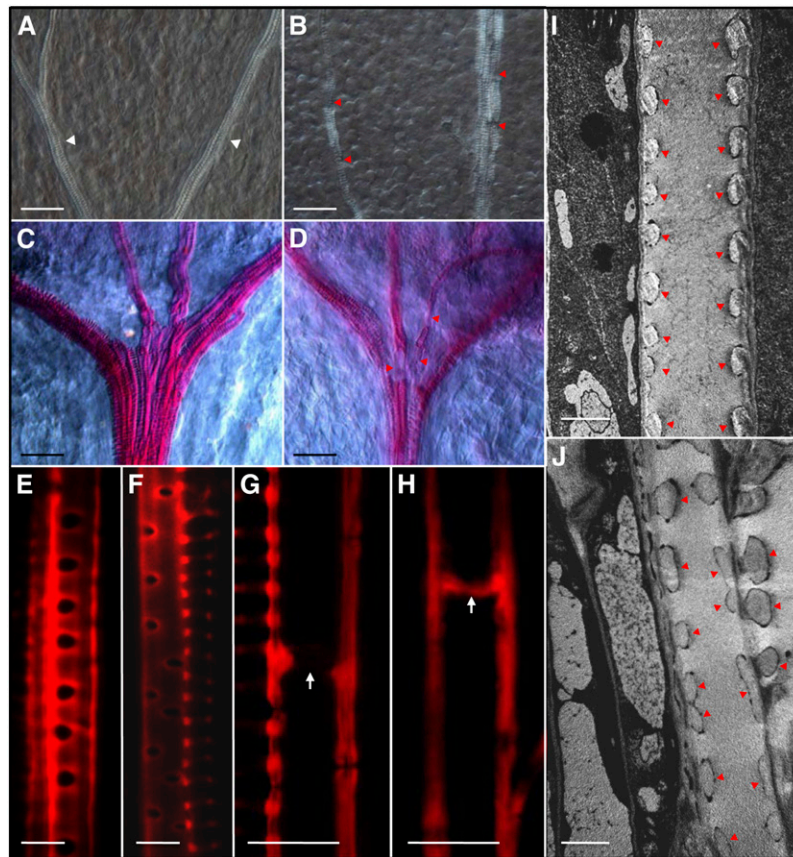
Figure 7. Defective TE Formation in *exo70a1-1* Seedlings.

(A) and **(B)** DIC images of cleared wild-type **(A)** and *exo70a1-1* **(B)** cotyledons of *Arabidopsis*. Note the gaps (red arrowheads) in TEs of *exo70a1-1* in contrast with continuous TEs (white arrowheads) in the wild type.

(C) and **(D)** Basic fuchsin staining of the cotyledon-hypocotyl junction regions from wild-type **(C)** and *exo70a1-1* **(D)** seedlings. Lignin-containing xylem is stained in bright pink. Note the lightly stained gaps (red arrowheads) in TEs.

(E) and **(F)** Mature metaxylem from wild-type **(E)** and *exo70a1-1* **(F)** roots, showing the pitted SCW pattern. Roots were stained with propidium iodide and observed under a confocal microscope. Note that pits in *exo70a1-1* were irregular.

(G) and **(H)** Perforations (white arrows) between two adjacent TEs in wild-type **(G)** and *exo70a1-1* **(H)** roots. Note that the perforation between two adjacent TEs in *exo70a1-1* was incomplete.

(I) and **(J)** TEM images of longitudinally sectioned mature protoxylem in wild-type **(I)** and *exo70a1-1* **(J)** hypocotyls. Note the irregular SCW thickenings (red arrowheads) on the side walls of TEs in *exo70a1-1*.

Bars = 25 μm in **(A)** to **(D)**, 5 μm **(E)** to **(H)**, and 2 μm in **(I)** and **(J)**.

2006). We showed that *exo70a1-1* plants exhibit severe defects in TE development, with reduced inner cell diameter, altered patterns of SCW thickening, and partial perforations. *EXO70G2* is another gene exhibiting a similar expression pattern to *EXO70A1* (Li et al., 2010), which may explain why a basic xylem system, with some abnormalities, is able to form in homozygous *exo70a1-1* plants. Mutations of both *EXO70A1* and *EXO70G2* may lead to

a complete loss of SCW thickening during TE differentiation and, consequently, to an embryo- or seedling-lethal phenotype.

Using ink transport experiments, we showed that the hydraulic transport efficiencies of inflorescence stems and roots of *exo70a1-1* are only approximately one-third of those in the wild type. Grafting of a wild-type root to the *exo70a1-1* shoot restores most aboveground defects, such as sterility, reduced

Table 1. Properties of Mature TEs

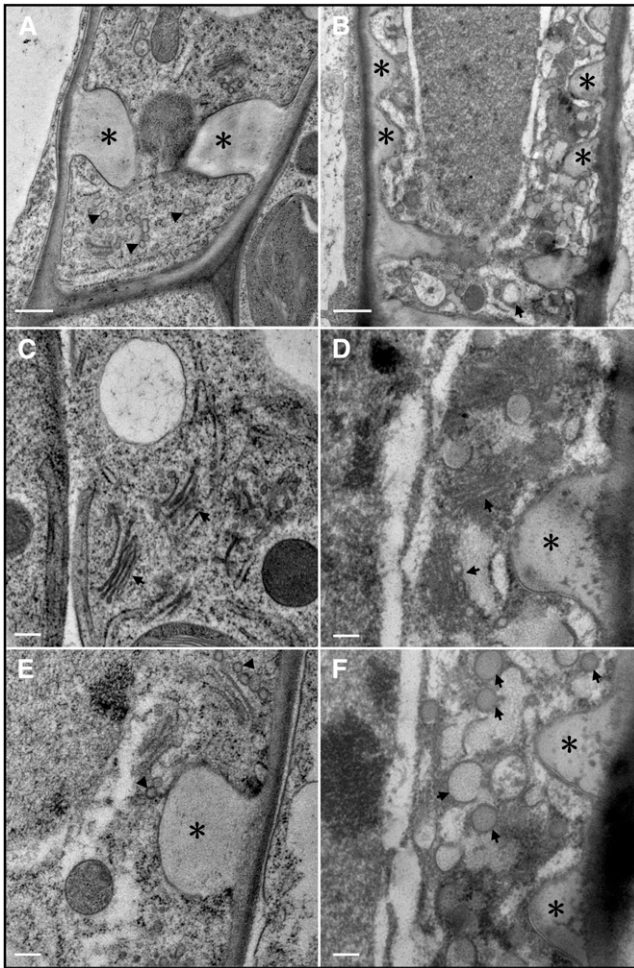| Genotype/P Value	Width of Perforations (μm)	Inner Diameters of TEs (μm)	Length of TEs (μm)	Pit Sizes (μm²)	Distance between Pits (μm)
The wild type	3.16 ± 1.16 (*n* = 32)	4.70 ± 1.30 (*n* = 28)	248.42 ± 107.58 (*n* = 30)	2.56 ± 0.54 (*n* = 160)	6.15 ± 0.79 (*n* = 150)
exo70a1-1	1.46 ± 1.54 (*n* = 30)	4.16 ± 1.16 (*n* = 36)	261.92 ± 107.08 (*n* = 30)	2.10 ± 0.56 (*n* = 171)	8.46 ± 0.85 (*n* = 150)
P value	<0.01	<0.01	>0.05	>0.05	<0.01

Figure 8. Cryo-Fixation and Electron Microscopic Observations of Developing TEs.

The junction regions between cotyledons and the hypocotyl, where new TEs are continuously formed, were examined. **(A)**, **(C)**, and **(E)**, the wild type; **(B)**, **(D)**, and **(F)**, *exo70a1-1*.
(A) and **(B)** Developing TEs in the wild type **(A)** and *exo70a1-1* **(B)**. Note the large membrane-bound compartment (arrow) in *exo70a1-1* compared with small vesicles in the wild type (arrowheads). Patterned SCW thickenings are marked with asterisks.
(C) and **(D)** Golgi bodies (arrows) in developing TEs of the wild type **(C)** and *exo70a1-1* **(D)**. Note the deformed Golgi bodies with an increased number of cisternae in *exo70a1-1*.
(E) and **(F)** Vesicles (arrowheads) in the developing TE of the wild type **(E)** compared with large membrane-bound compartments (arrows) in *exo70a1-1* **(F)**.
Bars = 0.5 μm in **(A)** and **(B)** and 0.2 μm in **(C)** to **(F)**.

organ expansion, and stigmatic papillae elongation. Nevertheless, ink transport experiments in grafted plants reveal that grafting a wild-type rootstock to an *exo70a1-1* shoot did not give a significant improvement of hydraulic transport in the inflorescence stem. We thus believe that the complementation of aboveground defects in W-m grafted plants is a consequence of improved water supply from the wild-type rootstock, which presumably leads to improved water delivery to the *exo70a1-1* inflorescence stem.

The short-root hair phenotype in *exo70a1-1* is more difficult to explain. Sufficient evidence shows that exocysts are involved in polarized growth in root hairs and pollen tubes. A mutation of maize *ROOTHAIRLESS1* that encodes a homolog of SEC3, another subunit of the exocyst complex, leads to severe deficiencies in root hair elongation (Wen and Schnable, 1994; Wen et al., 2005). A T-DNA insertion in *EXO70C1*, a gene expressed in pollen grains and pollen tubes, leads to a severe defect in pollen transmission (Li et al., 2010). However, because *EXO70A1* is not expressed in root hair cells and the exocyst is expected to act in a cell-autonomous manner, it is unlikely that the short root hair phenotype is caused directly by the mutation of *EXO70A1*. Actually, in addition to root hairs, we observed reduced cell expansion in many other cell types in roots, stems, and floral organs. It is plausible that the short-root hair phenotype is part of the general cell expansion defects caused by reduced hydraulic transport. Consistent with this, we observed severely reduced ink transport efficiency in the root of *exo70a1-1* plants. Of course, further experiments are needed in linking hydraulic transport to root hair elongation.

EXO70A1 Plays a Critical Role in Vesicle Trafficking in Developing TEs

The exocyst complex regulates the vesicle tethering process during exocytosis. As a key subunit of the exocyst complex, EXO70 in yeast interacts with Rho GTPases to regulate the polarized exocytosis and cell wall deposition (Robinson et al., 1999; He et al., 2007b; Wu et al., 2010). One thing peculiar in plants is the multiplication of *EXO70* genes in the genome (Synek et al., 2006). It remains to be answered whether these duplicated EXO70 members in plants act redundantly in exocytotic events or whether individual members have evolved specialized functions in specific cell types. Our studies support the latter proposition. Expression analyses of all 23 *EXO70* genes in *Arabidopsis* showed that individual *EXO70* members are expressed diversely in differentiating cells of various cell types, and none of these genes is expressed in fully differentiated cells such as mesophyll cells in mature leaves. This supports their hypothesized roles in regulating cell type– or cargo-specific vesicle trafficking (Li et al., 2010). In this study, we showed that mutation of *EXO70A1* resulted in irregular patterns of SCW thickening in TEs and abundant accumulation of large membrane-bound compartments specifically in developing TEs, although PCD, the final stage of TE differentiation, does not seem to be affected. These membrane-bound compartments, which may or may not be EXO70A1 positive, are significantly larger than wild-type exocytotic vesicles. The accumulation of such membrane-bound compartments is generally a sign of defective membrane trafficking, as for example in cytokinesis-defective mutants (Liu et al., 1995; Waizenegger et al., 2000). It has been shown previously that mutations in *EXO84B*, which encodes another subunit of the exocyst complex, lead to defective cytokinesis and accumulation of vesicles in epidermal cells in *Arabidopsis* (Fendrych et al., 2010). It is interesting to note that vesicles accumulated in the *exo84b* mutants are also much larger than the Golgi vesicles observed in the wild type (Fendrych et al., 2010). Of course, from these results, we cannot determine whether these larger membrane-bound compartments are on

their way to the plasma membrane, if they originate from fusions, or if an unconventional protein secretion pathway is involved (Ding et al., 2012).

In summary, these studies allowed us to propose that *EXO70A* in developing TEs regulates vesicle trafficking and patterned SCW thickening during TE formation. This is in agreement with the proposed hypothesis that individual EXO70 members in plants regulate cell type– or cargo-specific exocytosis (Li et al., 2010). The requirement of such a large number of *EXO70* genes in plants may be associated with dynamic functions of extracellular materials and communications between cells. Further functional characterization of other *EXO70* genes is needed to build an insightful connection between exocytosis and plant development.

METHODS

Plant Materials and Growth Conditions

T-DNA insertions in *exo70a1-1* and *exo70a1-2* were confirmed by PCR-based genotyping with T-DNA left border primer (LBa1, 5′-TGGTTCA-CGTAGTGGGCCATCG-3′) and *EXO70A1*-specific primers (5′-AAAAG-TATTTCTCCAGTTTTGGAAT-3′ and 5′-ATCGAATTGAGACAAAATAACT-TCA-3′ for *exo70a1-1* and 5′-GAGGCTTCGATTCTCTAAGT-3′ and 5′-TTGTACTGTTTCGATTTTCC-3′ for *exo70a1-2*). The selected homozygous *exo70a1-1* plant was backcrossed three times with the wild-type (*Arabidopsis thaliana* Columbia-0) to confirm the genetic linkage. For growth of seedlings on plates, seeds were gas sterilized and sown on solid media containing half-strength Murashige and Skoog mineral salts (Duchefa), 1% Su, 0.1% MES, and 1.5% agar, pH 5.7, and kept at 4°C in the dark for 3 d prior to transfer to a growth room and being cultivated vertically under long-day conditions (16 h light, 8 h darkness) at 21 ± 1°C. For growth in soil, 5-d-old seedlings on plates were transferred to pots filled with a soil-vermiculite mixture (1:1) under the same conditions.

Grafting Experiments

Grafting was performed using the method described previously (Turnbull et al., 2002) with some modifications. Wild-type and *exo70a1-1* seedlings cultivated in vertical plates for 3 d were cut perpendicularly at the upper quarter of the hypocotyls using a double-sided blade and rejoined using split 1-μL pipette tips as the supporting collar. The grafted seedlings were cultured in vertical plates for another 7 d before being transferred to soil and grown as described above.

Microscopy

GUS assays were performed as described previously (Li et al., 2010). For semithin sections, 10-d-old seedlings were fixed in a modified formalin-acetic acid solution (Liu et al., 1993) and embedded in LR White resin as described in the manufacturer's manual (London Resin Company). One-micrometer-thick sections were cut with a microtome and stained using periodic acid and Schiff's reagent (Sigma-Aldrich) for polysaccharides or toluidine blue for the general cellular structure (Sigma-Aldrich). For lignin visualizations, 7-d-old seedlings were cleared and stained with 0.01% basic fuchsin as described previously (Dharmawardhana et al., 1992). For observation of TEs, roots of 7-d-old seedlings were stained with 0.5 μg/mL propidium iodide solution (Sigma-Aldrich) for 5 min and then visualized under a confocal scanning microscope (Leica SP5). For observation of pollen tubes, 10 h after pollination, pistils were excised and fixed in a cold ethanol/acetic acid (3/1) solution for 1 to 3 h and then washed three times with distilled water, followed by incubation in 8 M NaOH overnight. These pistils were then washed in distilled water at least three times for 1 h each and then stained in 0.1% aniline blue in 0.1 M K_2HPO_4-KOH buffer for 30 min and observed under a fluorescence microscope (Leica DM4500B).

Cryo-Fixation and Electron Microscopy

Excised samples of the cotyledon-hypocotyl junction regions from 3-d-old seedlings were rapidly frozen using a High-Pressure Freezing Machine (Leica EM PACT2 with Leica EM RTS) at 2050 bars and stored under liquid nitrogen. Samples were freeze substituted in acetone containing 2% OsO_4 and 1% distilled water at −140°C. The temperature was gradually raised to −90°C over 2 h. The substitution was then performed according to following procedure: −90°C for 48 h, −60°C for 24 h, and −30°C for 24 h. After warming to 0°C, samples were washed three times in acetone and allowed to reach room temperature. These samples were then infiltrated with gradually increasing percentages of Spurr's resin (EMS) in acetone and embedded into flat modules. The resin was hardened by incubation at 70°C for 12 h. Section was performed with a microtome (Leica UC6), and observation was performed under a Philips-FEI TECNAI20 transmission electron microscope.

Physiological Assays

Water potentials were measured in 5-week-old plants using a vapor pressure osmometer (HR-33T, Wescor) by following the manual provided by the supplier. Water content was calculated by subtracting the weight of fully expanded, dried leaves from the fresh weight of the same leaves. For calculation of water loss rates, fully expanded leaves were excised and placed in a Petri dish and allowed to air dry. These leaves were weighed at different time points.

The hydraulic conductance assay was performed in stems using an ink transport experiment. The young inflorescence stems, 2 cm in length, were excised from 5-week-old wild-type and *exo70a1-1* plants, in which all postanthesis siliques were removed, keeping flowers and floral buds. The bottom ends of the stems were soaked in 1:5 diluted red ink (Pelikan). Under a dissection microscope, we monitored how long it took for the ink to reach the first flower or floral bud.

To measure the hydraulic transport in roots, two agarose blocks were prepared using half-strength Murashige and Skoog salts with 1% Suc and 1.5% agarose, one with 2:5 diluted blue ink (Pelikan) and another one without ink. These blocks were placed 1 mm apart in a 5-cm Petri dish. Eight-day-old wild-type and *exo70a1-1* seedlings (the length of primary roots is between 2.2 and 2.4 mm) were laid onto the surfaces of these blocks, with the root tip (~2 mm) on the ink block, and the rest of the seedling on the non-ink block. The distance of the ink transport is ~2 cm for all roots. We monitored how long it took for the ink to reach the hypocotyl under a dissection microscope.

For assisted pollinations, wild-type and *exo70a1-1* floral buds were emasculated and pollinated with pollens from wild-type and *exo70a1-1* plants in different cross combinations, and seed sets were counted after 2 weeks.

Measurements of Mineral Content

Minerals in aboveground tissues of 50-d-old wild-type and *exo70a1-1* plants were extracted and quantified using inductively coupled plasma–mass spectrometry as described by Gong et al. (2003).

Accession Numbers

The Arabidopsis Genome Initiative locus identifier for *EXO70A1* is At5g03540. T-DNA insertion lines, *exo70a1-1* (*Salk_014826*) and *exo70a1-2* (*Salk_135462*), were obtained from the ABRC.

Supplemental Data

The following materials are available in the online version of this article.

Supplemental Figure 1. *EXO70A1* Is Expressed in Developing TEs.

Supplemental Figure 2. *exo70a1-1*Plants Exhibit Dwarf, Reduced Organ Size and Nearly Sterile Phenotypes.

Supplemental Figure 3. Mineral Contents in Aboveground Tissues from Wild-Type and *exo70a1-1* Plants.

Supplemental Figure 4. Reduced Cell and Organ Expansion in *exo70a1-1*.

Supplemental Figure 5. Defective Stigmatic Papillae Elongation in *exo70a1-1* Can Be Rescued by W-m Grafting.

Supplemental Figure 6. Defective TE Development in *exo70a1-1* Hypocotyls.

Supplemental Figure 7. Patterned SCW Thickening at the Perforation Site in *exo70a1-1*.

AUTHOR CONTRIBUTIONS

S.L. and M.C. performed most of the research, and S.L. drafted the article. D.Y. carried out grafting experiments. S.R. performed some expression and ink transport analyses. S.S. carried out high-pressure freezing and freeze substitution. L.L. carried out electron microscopy analysis. T.K. and A.-M.C.E. supervised part of this project and revised the article. C.-M.L. designed the experiment, supervised the study, and revised the article.

REFERENCES

Bollhöner, B., Prestele, J., and Tuominen, H. (2012). Xylem cell death: Emerging understanding of regulation and function. J. Exp. Bot. **63:** 1081–1094.

Boyd, C., Hughes, T., Pypaert, M., and Novick, P. (2004). Vesicles carry most exocyst subunits to exocytic sites marked by the remaining two subunits, Sec3p and Exo70p. J. Cell Biol. **167:** 889–901.

Chong, Y.T., Gidda, S.K., Sanford, C., Parkinson, J., Mullen, R.T., and Goring, D.R. (2010). Characterization of the *Arabidopsis thaliana* exocyst complex gene families by phylogenetic, expression profiling, and subcellular localization studies. New Phytol. **185:** 401–419.

Cole, R.A., Synek, L., Zarsky, V., and Fowler, J.E. (2005). SEC8, a subunit of the putative *Arabidopsis* exocyst complex, facilitates pollen germination and competitive pollen tube growth. Plant Physiol. **138:** 2005–2018.

Cvrčková, F., Grunt, M., Bezvoda, R., Hála, M., Kulich, I., Rawat, A., and Zárský, V. (2012). Evolution of the land plant exocyst complexes. Front. Plant Sci. **3:** 159.

Dharmawardhana, D., Ellis, B., and Carlson, J. (1992). Characterization of vascular lignification in *Arabidopsis thaliana*. Can. J. Bot. **70:** 2238–2244.

Ding, Y., Wang, J., Wang, J., Stierhof, Y.D., Robinson, D.G., and Jiang, L. (2012). Unconventional protein secretion. Trends Plant Sci. **17:** 606–615.

Drdová, E.J., Synek, L., Pečenková, T., Hála, M., Kulich, I., Fowler, J.E., Murphy, A.S., and Zárský, V. (2013). The exocyst complex contributes to PIN auxin efflux carrier recycling and polar auxin transport in *Arabidopsis*. Plant J. **73:** 709–719.

Elias, M., Drdova, E., Ziak, D., Bavlnka, B., Hala, M., Cvrckova, F., Soukupova, H., and Zarsky, V. (2003). The exocyst complex in plants. Cell Biol. Int. **27:** 199–201.

Fendrych, M., Synek, L., Pecenková, T., Toupalová, H., Cole, R., Drdová, E., Nebesárová, J., Sedinová, M., Hála, M., Fowler, J.E., and Zárský, V. (2010). The *Arabidopsis* exocyst complex is involved in cytokinesis and cell plate maturation. Plant Cell **22:** 3053–3065.

Finger, F.P., Hughes, T.E., and Novick, P. (1998). Sec3p is a spatial landmark for polarized secretion in budding yeast. Cell **92:** 559–571.

Fukuda, H. (1997). Tracheary element differentiation. Plant Cell **9:** 1147–1156.

Fukuda, H. (2004). Signals that control plant vascular cell differentiation. Nat. Rev. Mol. Cell Biol. **5:** 379–391.

Gong, J.M., Lee, D.A., and Schroeder, J.I. (2003). Long-distance root-to-shoot transport of phytochelatins and cadmium in *Arabidopsis*. Proc. Natl. Acad. Sci. USA **100:** 10118–10123.

Haigler, C.H., and Brown, R.M. (1986). Transport of rosettes from the Golgi apparatus to the plasma membrane in isolated mesophyll cells of *Zinnia elegans* during differentiation to tracheary elements in suspension culture. Protoplasma **134:** 111–120.

Hála, M., Cole, R., Synek, L., Drdová, E., Pecenková, T., Nordheim, A., Lamkemeyer, T., Madlung, J., Hochholdinger, F., Fowler, J.E., and Zárský, V. (2008). An exocyst complex functions in plant cell growth in *Arabidopsis* and tobacco. Plant Cell **20:** 1330–1345.

He, B., and Guo, W. (2009). The exocyst complex in polarized exocytosis. Curr. Opin. Cell Biol. **21:** 537–542.

He, B., Xi, F., Zhang, J., TerBush, D., Zhang, X., and Guo, W. (2007a). Exo70p mediates the secretion of specific exocytic vesicles at early stages of the cell cycle for polarized cell growth. J. Cell Biol. **176:** 771–777.

He, B., Xi, F., Zhang, X., Zhang, J., and Guo, W. (2007b). Exo70 interacts with phospholipids and mediates the targeting of the exocyst to the plasma membrane. EMBO J. **26:** 4053–4065.

Kimura, S., Laosinchai, W., Itoh, T., Cui, X., Linder, C.R., and Brown, R.M., Jr., (1999). Immunogold labeling of rosette terminal cellulose-synthesizing complexes in the vascular plant *Vigna angularis*. Plant Cell **11:** 2075–2086.

Kitashiba, H., Liu, P., Nishio, T., Nasrallah, J.B., and Nasrallah, M.E. (2011). Functional test of *Brassica* self-incompatibility modifiers in *Arabidopsis thaliana*. Proc. Natl. Acad. Sci. USA **108:** 18173–18178.

Kubo, M., Udagawa, M., Nishikubo, N., Horiguchi, G., Yamaguchi, M., Ito, J., Mimura, T., Fukuda, H., and Demura, T. (2005). Transcription switches for protoxylem and metaxylem vessel formation. Genes Dev. **19:** 1855–1860.

Kulich, I., Cole, R., Drdová, E., Cvrčková, F., Soukup, A., Fowler, J., and Zárský, V. (2010). *Arabidopsis* exocyst subunits SEC8 and EXO70A1 and exocyst interactor ROH1 are involved in the localized deposition of seed coat pectin. New Phytol. **188:** 615–625.

Liu, C.M., Johnson, S., and Wang, T.L. (1995). *cyd*, a mutant of pea that alters embryo morphology is defective in cytokinesis. Dev. Genet. **16:** 312–331.

Liu, C.M., Xu, Z., and Chua, N.H. (1993). Auxin polar transport is essential for the establishment of bilateral symmetry during early plant embryogenesis. Plant Cell **5:** 621–630.

Li, S., van Os, G.M., Ren, S., Yu, D., Ketelaar, T., Emons, A.M., and Liu, C.M. (2010). Expression and functional analyses of *EXO70* genes in *Arabidopsis* implicate their roles in regulating cell type-specific exocytosis. Plant Physiol. **154:** 1819–1830.

Lucas, W.J., et al. (2013). The plant vascular system: Evolution, development and functions. J. Integr. Plant Biol. **55:** 294–388.

Milioni, D., Sado, P.E., Stacey, N.J., Domingo, C., Roberts, K., and McCann, M.C. (2001). Differential expression of cell-wall-related genes during the formation of tracheary elements in the *Zinnia* mesophyll cell system. Plant Mol. Biol. **47:** 221–238.

Oda, Y., and Fukuda, H. (2012). Initiation of cell wall pattern by a Rho- and microtubule-driven symmetry breaking. Science **337:** 1333–1336.

Pecenková, T., Hála, M., Kulich, I., Kocourková, D., Drdová, E., Fendrych, M., Toupalová, H., and Zársky, V. (2011). The role for the exocyst complex subunits Exo70B2 and Exo70H1 in the plant-pathogen interaction. J. Exp. Bot. **62:** 2107–2116.

Robinson, N.G., Guo, L., Imai, J., Toh-E, A., Matsui, Y., and Tamanoi, F. (1999). Rho3 of *Saccharomyces cerevisiae*, which regulates the actin cytoskeleton and exocytosis, is a GTPase which interacts with Myo2 and Exo70. Mol. Cell. Biol. **19:** 3580–3587.

Samuel, M.A., Chong, Y.T., Haasen, K.E., Aldea-Brydges, M.G., Stone, S.L., and Goring, D.R. (2009). Cellular pathways regulating responses to compatible and self-incompatible pollen in *Brassica* and *Arabidopsis* stigmas intersect at Exo70A1, a putative component of the exocyst complex. Plant Cell **21:** 2655–2671.

Smyth, D.R., Bowman, J.L., and Meyerowitz, E.M. (1990). Early flower development in *Arabidopsis*. Plant Cell **2:** 755–767.

Stegmann, M., Anderson, R.G., Ichimura, K., Pecenkova, T., Reuter, P., Žársky, V., McDowell, J.M., Shirasu, K., and Trujillo, M. (2012). The ubiquitin ligase PUB22 targets a subunit of the exocyst complex required for PAMP-triggered responses in *Arabidopsis*. Plant Cell **24:** 4703–4716.

Synek, L., Schlager, N., Eliás, M., Quentin, M., Hauser, M.T., and Zárský, V. (2006). AtEXO70A1, a member of a family of putative exocyst subunits specifically expanded in land plants, is important for polar growth and plant development. Plant J. **48:** 54–72.

Turnbull, C.G., Booker, J.P., and Leyser, H.M. (2002). Micrografting techniques for testing long-distance signalling in *Arabidopsis*. Plant J. **32:** 255–262.

Turner, S., Gallois, P., and Brown, D. (2007). Tracheary element differentiation. Annu. Rev. Plant Biol. **58:** 407–433.

Waizenegger, I., Lukowitz, W., Assaad, F., Schwarz, H., Jürgens, G., and Mayer, U. (2000). The *Arabidopsis KNOLLE* and *KEULE* genes interact to promote vesicle fusion during cytokinesis. Curr. Biol. **10:** 1371–1374.

Wang, J., Ding, Y., Wang, J., Hillmer, S., Miao, Y., Lo, S.W., Wang, X., Robinson, D.G., and Jiang, L. (2010). EXPO, an exocyst-positive organelle distinct from multivesicular endosomes and autophagosomes, mediates cytosol to cell wall exocytosis in *Arabidopsis* and tobacco cells. Plant Cell **22:** 4009–4030.

Wen, T.J., Hochholdinger, F., Sauer, M., Bruce, W., and Schnable, P.S. (2005). The *roothairless1* gene of maize encodes a homolog of *sec3*, which is involved in polar exocytosis. Plant Physiol. **138:** 1637–1643.

Wen, T.J., and Schnable, P.S. (1994). Analyses of mutants of three genes that influence root hair development in *Zea mays* (Gramineae) suggest that root hairs are dispensable. Am. J. Bot. **81:** 833–842.

Wu, H., Turner, C., Gardner, J., Temple, B., and Brennwald, P. (2010). The Exo70 subunit of the exocyst is an effector for both Cdc42 and Rho3 function in polarized exocytosis. Mol. Biol. Cell **21:** 430–442.

Yamaguchi, M., Goué, N., Igarashi, H., Ohtani, M., Nakano, Y., Mortimer, J.C., Nishikubo, N., Kubo, M., Katayama, Y., Kakegawa, K., Dupree, P., and Demura, T. (2010b). VASCULAR-RELATED NAC-DOMAIN6 and VASCULAR-RELATED NAC-DOMAIN7 effectively induce transdifferentiation into xylem vessel elements under control of an induction system. Plant Physiol. **153:** 906–914.

Yamaguchi, M., Kubo, M., Fukuda, H., and Demura, T. (2008). Vascular-related NAC-DOMAIN7 is involved in the differentiation of all types of xylem vessels in *Arabidopsis* roots and shoots. Plant J. **55:** 652–664.

Yamaguchi, M., Mitsuda, N., Ohtani, M., Ohme-Takagi, M., Kato, K., and Demura, T. (2011). VASCULAR-RELATED NAC-DOMAIN7 directly regulates the expression of a broad range of genes for xylem vessel formation. Plant J. **66:** 579–590.

Yamaguchi, M., Ohtani, M., Mitsuda, N., Kubo, M., Ohme-Takagi, M., Fukuda, H., and Demura, T. (2010a). VND-INTERACTING2, a NAC domain transcription factor, negatively regulates xylem vessel formation in *Arabidopsis*. Plant Cell **22:** 1249–1263.

Ye, Z.H. (2002). Vascular tissue differentiation and pattern formation in plants. Annu. Rev. Plant Biol. **53:** 183–202.

Zhang, Y., Immink, R., Liu, C.M., Emons, A.M., and Ketelaar, T. (March 18, 2013). The *Arabidopsis* exocyst subunit SEC3A is essential for embryo development and accumulates in transient puncta at the plasma membrane. New Phytol. http://dx.doi.org/10.1111/nph.12236.

Zhang, Y., Liu, C.M., Emons, A.M., and Ketelaar, T. (2010). The plant exocyst. J. Integr. Plant Biol. **52:** 138–146.